Functionalized gold nanorods as drug carriers: a promising antiviral system

Functionalized gold nanorods as drug carriers: a promising antiviral system

Elena Olivieri[1], Simone Amatori[1], Martina Marsotto[1], Giovanna Iucci[1], Chiara Battocchio[1], Maura Pellei[2], Carlo Santini[2], Andrea Cara[3], Zuleika Michelini[3], Marisa Colone[4], Annarica Calcabrini[4], Alessandra Paladini[5], Francesco Toschi[5], Iole Venditti[1*], Annarita Stringaro[4*]

[1] Sciences Department, Roma Tre University.via della Vasca Navale 79, 00146 Rome Italy
[2] School of Science and Technology, Chemistry Division, University of Camerino, via Madonna delle Carceri (ChIP), 62032 Camerino, Italy
[3] National Center for Global Health, Istituto Superiore di Sanità, Rome, Italy
[4] National Center for Drug Research and Evaluation, Istituto Superiore di Sanità, Rome, Italy
[5] CNR Istituto di Struttura della Materia - CNR (ISM-CNR), EuroFEL Support Laboratory (EFSL), Rome, Italy
iole.venditti@uniroma3.it: annarita.stringaro@iss.it

Abstract. Functionalized gold nanorods (AuNRs) are innovative tools useful in theranostics, combining diagnostics and therapy and allowing optimal and personal treatment of patients. Moreover, AuNRs are studied for use in photothermal therapy and imaging thanks to the peculiar phenomenon of Localised Surface Plasmon Resonance (LSPR), which allows them to be identified through spectroscopic techniques in the energy range in which biological tissues are not active. Their functionalization can involve a variety of molecules, including specific drugs or peptides, allowing a controlled transport and release of desired drugs. In this framework, AuNRs were synthesised and characterised through spectroscopic (UV–Vis-NIR, XPS) and microscopic techniques (TEM, FE-SEM). Furthermore, their cytotoxic activity was evaluated on Vero E6 cell line by MTT assay. The data obtained confirm the AuNRs are promising carriers for antiviral drugs, opening new possibilities of application for biomedical field.

1. Introduction

In medicine today, targeted and specific therapy is very important to reduce all possible side effects due to the use of high drug concentrations. It is also important to increase the efficiency of diagnosis in order to intervene rapidly. Functionalised gold nanorods (AuNRs) find numerous applications in the field of nanomedicine because they respond to these needs: AuNRs are innovative tools useful in "theranostics", the combination of diagnostics and therapy that allows an optimized and personalized treatment of patients with different pathologies [1-3]. This is due to the fact that they are versatile in their synthesis and possess peculiar chemical-physical properties. In particular, the AuNRs excitation involves the creation of the peculiar phenomenon of Localised Surface Plasmon Resonance (LSPR) due to the surface electron excitation, which allows them to be identified by spectroscopic techniques in the energy range where biological tissues are inactive. Specifically, the anisotropic shape induces two LSPR bands: the first is a transverse plasmon band corresponding to an electron oscillation along the short axis of the

rod, at around 520-550 nm and the second is a longitudinal plasmon band, in the range 600-1200 nm. Depending on the synthesis protocol used, AuNRs with different aspect ratios can be obtained [4-6].
Similar to all nanomaterials, the AuNRs functionalisation can involve a variety of molecules, including specific drugs, dyes or peptides, enabling controlled transport and release [7-14].
Moreover, in the last decade nanotechnology has demonstrated to be thriving to deliver essential changes to the development of antiviral therapeutics [15-19].
Lee et al. investigated a composite (functionalized AuNRs with hyaluronic acid and interferon α (HA-AuNP/IFNα)), which is an efficient drug delivery system, with long circulation times [20]. Indeed, after 7 days the composite was still in the murine liver tissue, inducing improvements in the innate immune system and a response to HCV infection in the liver tissue. Bai et al. prepared glutathione-stabilized fluorescent gold nanoclusters (AuNCs) that induce different antiviral effects on pseudorabies virus (PRV) and porcine reproductive and respiratory syndrome virus (PRRSV) [21]. Indeed these AuNCs could selectively inhibit the propagation of PRRSV (RNA virus) by direct virus inactivation and blockade of viral uptake but not that of PRV (DNA virus), which indicates the possibility of applying AuNCs in the treatment of infection by RNA viruses. More and more the development of new antiviral systems proceeds through the study of the virus in model cells, such as the Vero E6. In fact, these are particularly useful for studying the behavior of viruses and in particular of Corona viruses, because, as is well known, they do not produce interferon [22-24].
In this work hydrophilic AuNRs were synthesised by means of seed mediated method, using hexadecyltrimethylammonium bromide (CTAB) as stabilizer agent. The modulation of experimental parameters permits the aspect ratio (A.R.) control and good reproducibility. These AuNRs were analysed using X-ray photoelectron and Ultraviolet-visible-near spectroscopies (XPS and UV-Vis-NIR) and Transmission Electron Microscopy (TEM), which demonstrated their structure and morphological-ultrastructure respectively. Furthermore, cytotoxicity tests were performed on Vero E6 cell line in the presence of AuNRs to verify their low cytotoxic activity and to evaluate their use as carriers of antiviral agents.

2. Materials and methods

2.1. Materials

Cetyltrimethylammonium Bromide ($C_{19}H_{42}BrN$, CTAB, ≥ 97% Aldrich), tetrachloroauric acid ($HAuCl_4$ $3H_2O$, ≥ 99.9% Aldrich), sodium borohydride ($NaBH_4$, 99.99% Aldrich), silver nitrate ($AgNO_3$ 99.9%, Aldrich), L-ascorbic acid ($C_6H_8O_6$, 99% Sigma); the solvent used was double-distilled H_2O. Argon was used for degassing.
Vero E6 cell line used for cell viability assay derived from the kidney tissue of an adult African green monkey. This cell line was purchased from the American Type Culture Collection (ATCC) and was kindly provided by Dr. Andrea Cara from Istituto Superiore di Sanità (ISS). Cells were grown in DMEM (Euroclone) supplemented with 10% fetal bovine serum (FBS) (Corning), 1% penicillin (50 U-mL)-streptomycin (Gibco), 1% non-essential amino acids (Euroclone), 1% sodium pyruvate (Gibco) at 37°C and in an atmosphere containing 5% CO_2 and sub-cultured at confluence.

2.2 Instruments

Ultraviolet-visible spectroscopy (UV–Vis-NIR) spectra were recorded with a Shimadzu 2401 PC UV-Vis spectrophotometer and using quartz cuvettes with an optical path of 1 cm. The X-ray Photoelectron Spectroscopy XPS analysis was performed with a home-made instrument, consisting of preparation and ultra-high vacuum (UHV) analysis chambers separated by a slide valve. The analysis chamber is equipped with a six-degree-of-freedom manipulator and a 150-mm mean radius hemispherical electron analyser with a five-lens output system combined with a 16-channel detector providing a total instrument resolution of 1.0 eV measured at the Ag 3d5/2 core level. The samples were introduced into the preparation chamber and allowed to degas overnight at a base pressure of approximately 10^{-8} Torr, prior to introduction into the analysis chamber. The X-ray radiation used was a non-monochromatic Mg Kα

(1253.6 eV). The spectra were referred to the C1s signal energy of aliphatic C atoms having a binding energy BE = 285.0 eV. Atomic ratio values were calculated from the peak intensities. Curve-fitting analysis of the C1s, N1s and O1s spectra was performed using Gaussian profiles as fitting functions, after subtraction of a polynomial background.
The morphological-ultrastructural analysis of AuNRs was performed using a transmission electron microscope (TEM) (Philips EM 208S, FEI Company, Eindhoven, The Netherlands) with a tungsten source and magnification power up to 200K, equipped with a MegaView III camera (Olympus Soft Imaging Solutions) for image acquisition. A suspension drop of AuNRs was deposited on a formvar-carbon coated copper grid for subsequent TEM observations.

2.3 AuNRs synthesis
0.2 M CTAB solution, 0.0005 M, 0.001 M $HAuCl_4$ solution and 0.01 M $AgNO_3$ solution and 0.078M ascorbic acid (AA) solution were prepared. The synthesis procedure followed seed mediated method, in two steps. First step: 5 mL of CTAB (0.2 M) and 5 mL of $HAuCl_4$ (0.0005 M) were placed in a 100 mL flask equipped with a magnetic stirring rod and degassed for 5 minutes with Ar. After $NaBH_4$ was added (600 µL, 0.01 M) and stirred for a further 5 minutes. Second step: CTAB (5 mL, 0.2 M) $HAuCl_4$ (5 mL, 0.001 M) and $AgNO_3$ (200 µL, 0.004 M) were added in a 100 mL flask and degassed for 5 minutes with Ar. Then ascorbic acid (70 µL, 0.078 M) and seed solution (24 µL) were added. The reaction continues to be stirred regularly (500 rpm) for 20 minutes. To purify AuNRs, two centrifugations were performed at 13,000 rpm for 15 minutes.

2.4 Cell viability assay
Vero E6 cell viability was analysed by MTT (3-(4,5-dimethylthiazol-2-yl)-2,5-diphenyltetrazolium bromide) assay according to the following protocol.
Cells were seeded into 96-well microtiter plates (NunclonTM, Nunc, Germany) at density of $1.8*10^4$ in a volume of 200 µL per well. After 24 h cells were treated with 0.05 µg/mL of AuNRs. After an incubation period of 24, 48 and 72 h, medium was replaced by new fresh containing 0.5mg/mL MTT (Sigma, Deisenhofen, Germany). After 2 h at 37°C, unreacted dye was removed and the purple formazan product was dissolved in 200 µl/well dimethylsulfoxide (Merck, Darmstadt, Germany). Absorbance was read at 570 nm by using the Fusion Universal Microplate Analyzer (Packard BioScience Company, Connecticut, USA) supplied at the ISS. The data were expressed as absorbance relative to untreated cells in the same experiment and standardized to 100%. All data points were performed in triplicate. Results (average of two to three experiments) are expressed as mean ± standard error. Statistical analysis of the data was performed using Graph Pad PRISM software.

3. Results and discussions

3.1 AuNRs synthesis and characterizations
For the synthesis, the experimental protocol reported in the work of Nikoobakht et al. was followed [25]. This type of synthesis allowed good control of the shape and size of the AuNRs and thus the achievement of a stable, low-dispersion and reproducible synthesis. The protocol involves the synthesis in two steps. In the first step, the seed solution, the solution containing the nucleation seeds, is synthesised. In the second step, the growth solution run: rod growth begins 10 minutes after the addition of the seed solution to the growth solution. It is evident how, as the rod grows, there is a change in the colour of the reaction mixture from transparent, due to the reduction of gold by ascorbic acid, to pinkish, which intensifies over time to a violet-blue colour [26]. In this second step, silver nitrate is added and aids anisotropic rod growth [27]. To assess the chemical composition and structure of the AuNRs XPS experiments were performed at the C1s, N1s, Ag3d and Au4f core levels on the sample deposited onto a TiO_2/Si(111) wafer surface following a drop-casting procedure. The C1s, N1s, Ag3d and Au4f spectra (Figure 1) were analysed following a peak-fitting procedure, allowing components from chemical elements with different atomic environment to be identified; all binding energy (BE) peak positions, full width at half

maximum (FWHM), atomic ratio (relative intensities) values and proposed assignments are reported in Table 1. The C1s spectrum (Figure 1a) appears to be composite, and at least four spectral components can be identified by following a peak-fitting procedure: the peak at lower BE (285.0 eV) is due to aliphatic C-C ascorbate groups and impurities, always found on samples prepared in air; the peaks at about 286.4 and 287.8 eV are attributed to C-OH and C=O (ascorbate functional groups); the contribution at 289.2 eV is attributed to COOH impurities on the sample surface [28]. The N1s spectrum (Figure 1b) has two components: the first at lower BE is associated with C-N nitrogens, the other at about 400.0 eV, with the protonated nitrogen of CTAB [29]. The Au4f spectrum (Figure 1c) shows two spin-orbit pairs ($Au4f_{7/2}$, $Au4f_{5/2}$) doublets, of which we take $Au4f_{7/2}$ as the reference. The $Au4f_{7/2}$ signal around 83.7 eV is due to the metallic gold atoms at the bulk of AuNRs, while the $Au4f_{7/2}$ component at 84.2 eV is indicative for positively charged Au atoms at the nanorod surface [30]. As for Ag3d spectrum (Figure 1d), the $Ag3d_{5/2}$ signal at 367.3 eV is attributed to Ag(I) ions and the low-intensity signal around 368.1 eV to a low amount of metallic Ag atoms, as suggested by the literature on analogous systems [31].

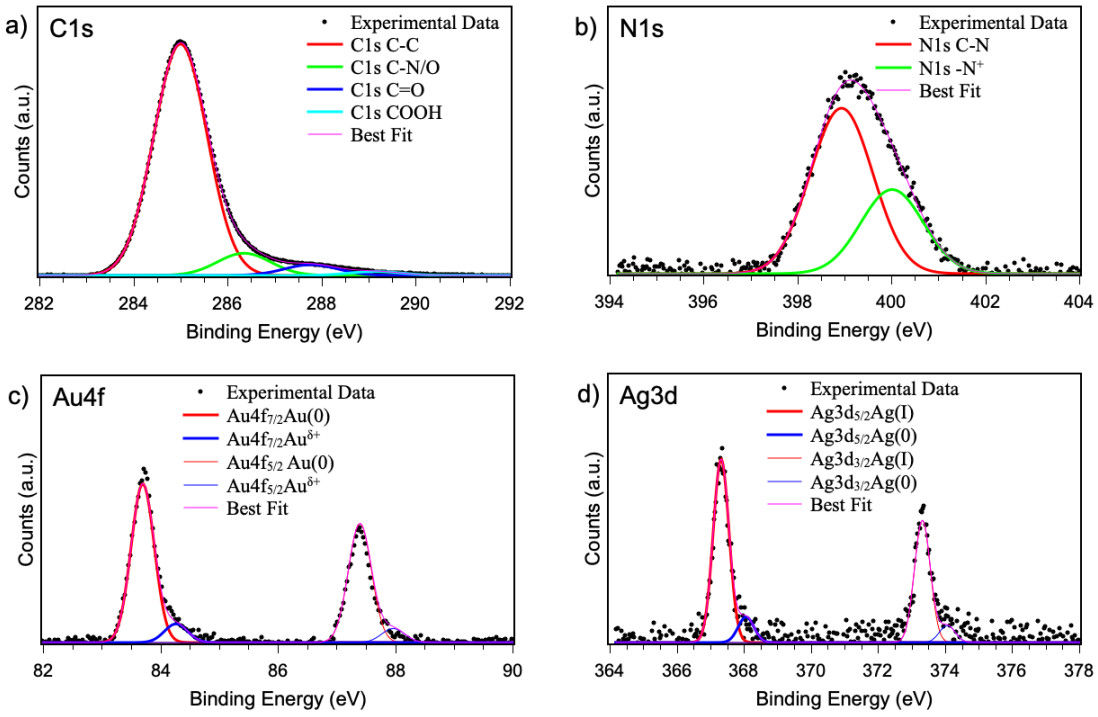

Figure 1. *XPS spectra C1s (a), N1s (b), Au4f (c), Ag3d (d).*

Table 1. *XPS data analysis results.*

Signal	Assignment	FWHM	BE (eV)	Atomic Ratios (%)
C1s	C-C	1.34	285.00	86
	C-N/C-O		286.35	8
	C=O		287.78	4
	COOH		289.15	2

N1s	C-N $-N^+$	1.57	398.94 400.02	66 34
Ti2p	TiO_2	1.17	458.47	100
Ag3d	Ag^0 $Ag^{\delta+}$	0.56	367.32 368.07	88 12
Au4f	Au^0 $Au^{\delta+}$	0.47	83.70 84.27	90 10

Through the UV-Vis spectrum, the correct longitudinal growth of the rods can be assessed. In fact, as shown in Figure 2, the presence of two plasmons, one around 515 nm, the other around 745 nm, confirms that growth has occurred.

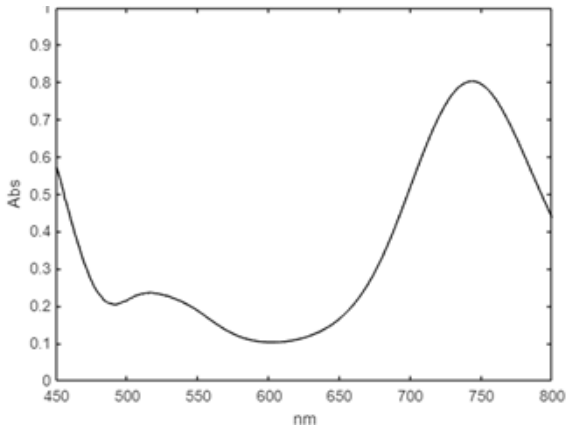

Figure 2. Uv-Vis spectrum of AuNRs, with the two LSPR at λ_{max} 515 nm and 745 nm.

To assess the aspect ratio of the AuNRs, TEM images were acquired. In Figure 3 TEM image of AuNRs with average size 39 ± 4 x 12 ± 5 nm was shown. The aspect ratio calculated for the AuNRs used is 3.2 nm.

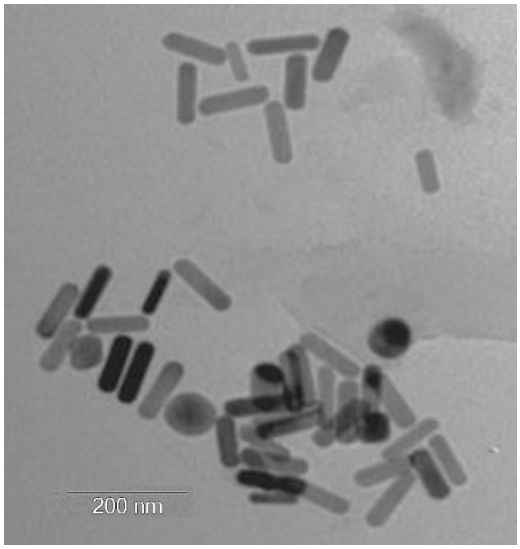

Figure 3. *TEM image* of AuNRs with *A.R= 3.2 nm.*

3.2 Biological tests

To study the biocompatibility of AuNRs, Vero E6 cell viability was assessed after treatment with 0.05 µg/mL solutions for 24, 48 and 72 h. The results shown in Figure 4 indicate that AuNRs at this concentration did not induce any significant reduction in cell viability at all incubation times, on the contrary, they appeared highly biocompatible. This result demonstrated a promising behaviour of AuNRs, employed at this concentration.

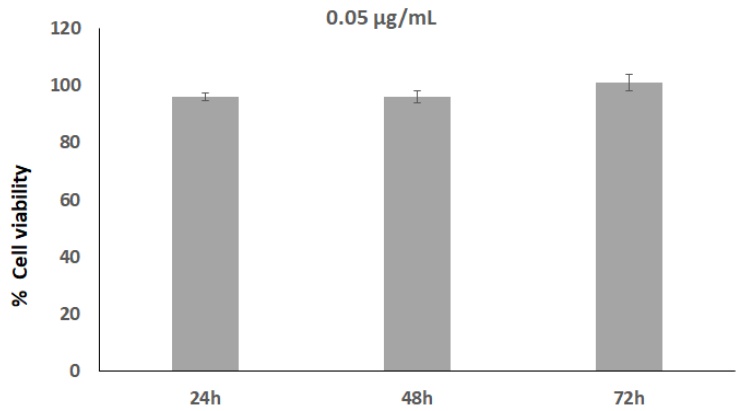

Figure 4. MTT assay: Vero E6 cell viability percentage (referred to 100% untreated cell viability) after treatment with 0.05 µg/mL AuNRs at different times.

4. Conclusions

In this work AuNRs were prepared by seed-mediated synthesis, in two steps, obtaining nanodimensions verified by TEM analysis of 39 ± 4 x 12 ± 5 nm nm, with A.R. = 3.2 The morphology and size was verified by UV-Vis-NIR spectroscopy, highlighting the two plasmonic peaks at λ_{max} 515 nm and 745 nm. Furthermore, the structural study using XPS confirmed the stability of the system. Cell survival studies have been conducted with AuNRs and Vero E6 cells, used in testing for antivirals. These studies have allowed us to highlight the biocompatibility of AuNRs at a concentration of 0.05 µg/mL, opening up promising prospects in the transport of antiviral drugs.

Author Contributions: Conceptualization, I.V. and A.R.S; methodology E.O, S.A. M.M. C.B. C.S. M.P. A.P.; E.O., S.A. and I.V. designed and performed the AuNRs synthesis and UV–Vis measurements and evaluations. E.O., M.C., A.C., A.C., Z.M. and A.R.S. performed the biological tests. XPS measurements and the data analysis were performed by M.M., G.I. and C.B.; A.P. and F. T. performed the UV-Vis-NIR measurements and the data analysis. All authors contributed to the paper writing and revision. All authors have read and agreed to the published version of the manuscript.

Acknowledgments
The Grant of Excellence Departments, MIUR (ARTICOLO 1, COMMI 314–337 LEGGE 232/2016), is gratefully acknowledged by authors of Roma Tre University. The authors of the Science Department of the University of Roma Tre and of the CNR recognize the support of the Framework Agreement signed between the CNR and the University of Roma Tre, on 24 September 2019. This work was supported by grants from Unione Europea - NextGenerationEU, "MUR - Fondo Promozione e Sviluppo - D.M. 737/2021, *An innovative platform against SARS-CoV-2 and other emerging viruses grounded on copper-based materials (INVIRCuM)*".

Conflicts of Interest: The authors declare no conflict of interest.

References

[1] Ding X, Li D., J. Jiang; Gold-based Inorganic Nanohybrids for Nanomedicine Applications; Theranostics, 2020, 10, 8061–8079.
[2] X. Chen, S. S. Gambhir, J. Cheon; Theranostic Nanomedicine, Acc. Chem. Res. 2011, 44, 841.
[3] D. Maccora, V. Dini, C. Battocchio, I. Fratoddi, A. Cartoni, D. Rotili, M. Castagnola, R. Faccini, I. Bruno, T. Scotognella, A. Giordano, I. Venditti; Gold nanoparticles and nanorods in nuclear medicine: a mini review; Applied Sciences, 2019, 9 (16), 3232
[4] V. Sharma, K. Park, M. Srinivasarao; Colloidal dispersion of gold nanorods: Historical background, optical properties, seed-mediated synthesis, shape separation and self-assembly; Materials Science and Engineering R, 2009, 65, 1-38.
[5] X. Wena, H. Shuaib, L. Min; Precise modulation of gold nanorods aspect ratio based on localized surface plasmon resonance; Optical Materials, 2016, 60, 324-330.
[6] J. Wan, J. H. Wang, T. Liu, Z. Xie, X. F.Yu, W. Li; Surface chemistry but not aspect ratio mediates the biological toxicity of gold nanorods in vitro and in vivo; Sci. Rep., 2015, 5, 11398.
[7] I. Venditti, G. Iucci, I. Fratoddi, M. Cipolletti, E. Montalesi, M. Marino, V. Secchi, C. Battocchio; Directly Resveratrol immobilization on hydrophilic charged gold nanoparticles: structural investigations and cytotoxic studies; Nanomaterials, 2020, 10(10), 1898.
[8] K. Bouchemal; New challenges for pharmaceutical formulations and drug delivery systems characterization using isothermal titration calorimetry; Drug Discovery Today, 2008, 13, 21.
[9] I. Fratoddi, I. Venditti, C. Battocchio, L. Carlini, M. Porchia, F. Tisato, F. Bondino, E. Magnano, M. Pellei, C. Santini; Highly hydrophilic gold nanoparticles as carrier for anticancer copper(I) complexes: loading and release studies for biomedical applications; Nanomaterials, 2019, 9, 772.
[10] C. Grabinski, N. Schaeublin, A. Wijaya, H. D'Couto, S. H. Baxamusa, K. Hamad-Schifferli, S. M. Hussai; Effect of Gold Nanorod Surface Chemistry on Cellular Response; ACS Nano, 2011, 5.4,2870–2879.
[11] I. Venditti, I. Fratoddi, C. Palazzesi, P. Prosposito, M. Casalboni, C. Cametti, C. Battocchio, G. Polzonetti, M. V. Russo; Self-assembled nanoparticles of functional copolymers for photonic applications; Journal of Colloids and Interface Science, 2010, 348, 424-430.
[12] U.A. Awan, A. Raza, S. Ali, R.F. Saeed, N. Akhtar; Doxorubicin-loaded gold nanorods: a multifunctional chemo-photothermal nanoplatform for cancer management; Nanotechnol., 2021, 12, 295-303.

[13] I. Venditti, N. Barbero, MV. Russo, A. Di Carlo, F. Decker, I. Fratoddi, C. Barolo, D. Dini; Electrodeposited ZnO with squaraine sentisizers as photoactive anode of DSCs; Materials Research Express, 2014, 1, 015040.
[14] Y. Xiao, H. Hong, V.Z. Matson, A. Javadi, W. Xu, Y. Yang, Y. Zhang, J. Engle, W., R.J. Nickles, W. Cai, D.A. Steeber, S. Gong; Gold Nanorods Conjugated with Doxorubicin and cRGD for Combined Anticancer Drug Delivery and PET Imaging; Theranostics, 2012, 2, 757–768.
[15] S. Szunerits, A. Barras, M. Khanal, Q. Pagneux, R. Boukherroub; Nanostructures for the Inhibition of Viral Infections; Molecules, 2015, 20.
[16] L. Chen, G. Huang; The antiviral activity of polysaccharides and their derivatives; Int. J. Biol.Macromol, 2018, 115, 77–82.
[17] F.D. Cojocaru, D. Botezat, I. Gardikiotis, C. M. Uritu, G. Dodi, L. Trandafir, C. Rezus, E. Rezus, I. B. Tamba, C. Mihai; Nanomaterials Designed for Antiviral Drug Delivery Transport across Biological Barriers, Pharmaceutics, 2020, 12, 1-34.
[18] A. Edouard; The Potential of Various Nanotechnologies for Coronavirus Diagnosis/Treatment Highlighted through a Literature Analysis; Bioconjugate Chemistry, 2020, 31 (8), 1873-1882.
[19] M.Y. Lee, J.A. Yang, H. S. Jung, S. Beack, J. E. Choi, W. Hur, H. Koo, K. Kim, S. K. Yoon, S. K. Hahn; Hyaluronic acid-gold nanoparticle/interferon α complex for targeted treatment of hepatitis C virus infection; ACS Nano, 2012, 6, 9522–9531.
[20] Y. Bai, Y. Zhou, H. Liu, L. Fang, J. Liang, S. Xiao; Glutathione-Stabilized Fluorescent Gold Nanoclusters Vary in Their Influences on the Proliferation of Pseudorabies Virus and Porcine Reproductive and Respiratory Syndrome Virus; ACS Appl. Nano Mater., 2018, 1, 969–976.
[21] O. Naoki, K. Arihiro, Y. Toshiyuki, H. Noriko, K. Fumio, S. Tsuyoshi, K. Makoto, H. Kentaro; The genome landscape of the african green monkey kidney-derived Vero cell line, DNA Res., 2014, 21, 673-683.
[22] L.D. Coimbra, A. Borin, M. Fontoura, H.D. Gravina, A. Nagai, J.F. Shimizu, K. Bispo-dos-Santos, F. Granja, P.S. L. Oliveira, K.G. Franchini, K. Samby, M. Bruder, J.L. Proenca-Modena, D.B.B. Trivella, J.H.C. Smetana, A.T. Cordeiro, R.E. Marques; Identification of Compounds With Antiviral Activity Against SARS-CoV-2 in the MMV Pathogen Box Using a Phenotypic High-Throughput Screening Assay, Frontiers, 2022, 2
[23] G.A. Pires De Souza, M. Le Bideau, C. Boschi, N. Wurtz, P. Colson, S. Aherfi, C. Devaux, B. La Scola; Choosing a cellular model to study SARS-CoV-2, Front. Cell. Infect. Microbiol., 2022, 12.
[24] S. Mariotti, A. Capocefalo, M.V. Chiantore, A. Iacobino, R. Teloni, M. L. De Angelis, A. Gallinaro, M.F. Pirillo, M. Borghi, A. Canitano, Z. Michelini, M. Baggieri, A. Marchi, P. Bucci, P.F. McKay, C. Acchioni, S. Sandini, M. Sgarbanti, F. Tosini, A. Di Virgilio,G. Venturi, F. Marino, V. Esposito, P. Di Bonito, F. Magurano, A. Cara, D. Negri, R. Nisini; Isolation and Characterization of Mouse Monoclonal Antibodies That Neutralize SARS-CoV-2 and Its Variants of Concern Alpha, Beta, Gamma and Delta by Binding Conformational Epitopes of Glycosylated RBD With High Potency; Frontiers in Immunology 2012, 12, 1226.
[25] Nikoobakht, B.; El-Sayed M.A.; Preparation and Growth Mechanism of Gold Nanorods (NRs) Using Seed-Mediated Growth Method; Chem. Mater., 2003, 15, 1957-1962.
[26] H. Chen, C. Xuemei, L. Bowen, Z. Min, M. Yuxiang, A. Samuel, G. Yueqing; Drug loaded multilayered gold nanorods for combined photothermal and chemotherapy; Biomater. Sci., 2014, 2, 996-1006.
[27] L. M. Moreau, M. Jones, E. Roth, J. Wu,, S. Kewalramani, M. N. O'Brien, B.R. Chen, C.A. Mirkin, M. Bedzyk; The role of trace Ag in the synthesis of Au nanorods; Nanoscale, 2019, 11, 11744–11754.
[28] G. Beamson, D. Briggs; High Resolution XPS of Organic Polymers: The Scienta ESCA 300 Database; John Wiley & Sons: Chichester, U.K., 1992, 70, A25.
[29] S. D. Techane, L. J. Gamble, D.G. Castner; X-ray photoelectron spectroscopy characterization of gold nanoparticles functionalized with amine-terminated alkanethiols; Biointerphases, 2011, 6, 98.
[30] I. Venditti, A. Cartoni, S. Cerra, R. Fioravanti, T. A. Salamone, F. Sciubba, M. A. Tabocchini, V. Dini, C. Battocchio, G. Iucci, L. Carlini, R. Faccini, F. Collamati, C. Mancini Terracciano, E. Solfaroli

Camillocci, S. Morganti, A. Giordano, T. Scotognella, D. Maccora, D. Rotili, C. Marchese, E. Anastasiadou, P. Trivedi, I. Fratoddi; Hydrophilic Gold Nanoparticles as anti-PD-L1 Antibody carriers: Synthesis and Interface Properties; Particle and Particle Systems Characterization, 2022, 39, 4.
[31] C. Oliveira, C. C. Ribeiro, B. Pascal, M. da Grac, C. Rocha, A. Ferreira da Silva Jos, F.D. Chubaci, M. Boström, C. Persson, M. Malta; Surface studies of the chemical environment in gold nanorods supported by X-ray photoelectron spectroscopy (XPS) and ab initio calculations; journal of materials research and technology, 2023, 23, 768-776.